Available online at www.sciencedirect.com
SCIENCE DIRECT®
Journal of Nuclear Materials 335 (2004) 508–514
journal of nuclear materials
www.elsevier.com/locate/jnucmat

Synergistic effects of implanted helium and hydrogen and the effect of irradiation temperature on the microstructure of SiC/SiC composites

T. Taguchi [a,*], N. Igawa [a], S. Miwa [b], E. Wakai [c], S. Jitsukawa [c]
L.L. Snead [d], A. Hasegawa [b]

[a] *Neutron Science Research Center, Japan Atomic Energy Research Institute, Tokai, Ibaraki 319-1195, Japan*
[b] *Department of Quantum Science and Energy Engineering, Tohoku University, Sendai, Miyagi 980-8579, Japan*
[c] *Department of Materials Science, Japan Atomic Energy Research Institute, Tokai, Ibaraki 319-1195, Japan*
[d] *Metals and Ceramics Division, Oak Ridge National Laboratory, P.O. Box 2008, Oak Ridge, TN 37831, USA*

Received 23 April 2004; accepted 31 August 2004

Abstract

The microstructure of near-stoichiometric fiber SiC/SiC composites implanted with He and H ions was studied at implantation temperatures of 1000 and 1300 °C. The average size of He bubbles in the CVI SiC matrix decreases with increasing concentration of implanted H ions. Moreover, the number density of He bubbles increases with increasing irradiation temperature and amount of implanted H. At the irradiation temperature of 1000 °C, He bubbles were mainly formed at grain boundary within the matrix. On the other hand, He bubbles were formed both at grain boundaries and within grains at the irradiation temperature of 1300 °C. The average size of He bubbles at grain boundaries was much larger than within the grain. The average size of He bubbles in the fiber was smaller than that in the matrix in all cases.

1. Introduction

Silicon carbide (SiC) fiber reinforced SiC matrix (SiC/SiC) composites are being developed as structural materials for fusion power reactors in part due to their high temperature strength and low-residual radioactivity following neutron irradiation [1–4]. It is reported that the SiC/SiC composites using highly crystalline and near-stoichiometric SiC fiber fabrics as reinforcement have excellent stability about microstructure and mechanical properties against neutron irradiation up to 20 dpa [5,6] However, the effect of transmutation gasses on SiC, which are not produced in the current fission-neutron damage studies, is largely unknown. Of particular concern are the high levels of helium (He) and hydrogen (H) transmutation atoms produced by the 14.1 MeV fusion neutrons. The production rates of He and H in SiC in first wall region are approximately 1500–2000 and 800 appm/MW-a/m^2 corresponding to a gas/dpa ratio

* Corresponding author. Tel.: +81 29 282 6099; fax: +81 29 282 5922.
E-mail address: taguchi@popsvr.tokai.jaeri.go.jp (T. Taguchi).

0022-3115/$ - see front matter
doi:10.1016/j.jnucmat.2004.08.014

of 130 appm He/dpa and 40 appm H/dpa [1]. Irradiation-induced microstructural and mechanical properties changes may be accelerated in SiC/SiC composites under the fusion condition since He is insoluble in virtually all materials and is captured easily within vacancy clusters produced during cascade formation.

Authors have previously reported that He bubbles in SiC/SiC composite with advanced SiC fiber were formed by simultaneous ion-beam irradiation with Si^{2+}, He^{+} and H^{+} ion-beams at 1000 °C [7]. The effects of He and H transmutation atoms on the formation of He bubbles, however, have not been thoroughly investigated. Additionally, it is also important to understand the effect of transmutation atoms on the microstructural change of SiC/SiC composites at higher temperature than 1000 °C, since the operational use temperature for SiC/SiC composite in a fusion reactor has been assumed to be around 1100 °C [1,5].

In this study, the effect of implanted He and H atoms and irradiation temperature on microstructural change of SiC/SiC composites using near-stoichiometric SiC fiber; Hi-Nicalon Type S and Tyranno SA, is presented by application of simultaneous ion irradiation at 1000 and 1300 °C.

2. Experimental procedure

2.1. Materials

The 2 D plane weave of Hi-Nicalon Type S and Tyranno SA SiC fiber fabrics as reinforcement were used in this study. The SiC/SiC composites were fabricated using the forced thermal gradient chemical vapor infiltration (F-CVI) process at Oak Ridge National Laboratory. The details of fabrication procedure are described elsewhere [8]. Carbon layer was deposited on the SiC fiber as an interphase layer between the matrix and the fiber. The matrix formed by this process consists of a highly pure, faulted form of β-SiC. Such composites typically have approximately 15% porosity. However, on the scale important for the microstructural studies presented here, the matrix can be considered fully dense and stoichiometric.

2.2. Irradiation

Simultaneous ion irradiation was carried out at TIARA (Takasaki Ion Accelerators for Advanced Radiation Application) facility of JAERI. The specimens were irradiated at 1000 or 1300 °C by 6.0 MeV Si^{2+} ions, 1.0 MeV He^{+} ions and/or 340 keV H^{+} ions. Various combinations of ions were examined in this study as summarized in Table 1. The implantation of He^{+} and H^{+} ions was conducted using an aluminum foil energy degrader in order to control He and H distribution in the depth range of about 1.0–1.8 μm from the specimen surface. The displacement damage, He, H and Si concentration as a function of depth from the surface in SiC calculated by TRIM code [9] is shown in Fig. 1. The displacement threshold energies of Si and C were assumed to be 35 and 20 eV, respectively [10]. The irradiation was performed to 10 dpa at the depth of 1.4 μm as shown in Fig. 1. The resultant He/dpa and H/dpa ratio were 130 and 40 appm/dpa, which would correspond to a region of the first wall of a fusion power reactor.

2.3. Microstructure observation

Focused ion beam processing was used to prepare thin foil specimens for transmission electron microscopy (TEM) observation. Microstructure observation was conducted with TEM (JEOL 2000 FX) operated at 200 kV.

3. Results and discussion

The low-magnification TEM microphotograph of the irradiated SiC/SiC composite by simultaneous triple ion-beams at 1300 °C is shown in Fig. 2. The SiC/SiC composites examined in this study have a 150 nm carbon layer as the interphase layer between fiber and matrix. Fiber/matrix interphase debonding, which leads the degradation of strength after irradiation [11,12], did not occur for all combination of ion-beams irradiation at both 1000 and 1300 °C in this study. Axial shrinkage of Hi-Nicalon SiC fibers, which are predecessor of advanced SiC fiber, was observed by ion irradiation at 1000 °C because of their re-crystallization [13]. The surfaces of the

Table 1
Irradiation condition of simultaneous ion-beams in this study

Condition ID	Kinds of ions	Displacement damage (dpa)	He concentration (appm)	H concentration (appm)
Single (Si)	Si^{2+}	10	0	0
Single (He)	He^{+}	∼0	1300	0
Dual	$Si^{2+} + He^{+}$	10	1300	0
Triple	$Si^{2+} + He^{+} + H^{+}$	10	1300	400
Triple (H × 10)	$Si^{2+} + He^{+} + H^{+}$	10	1300	4000

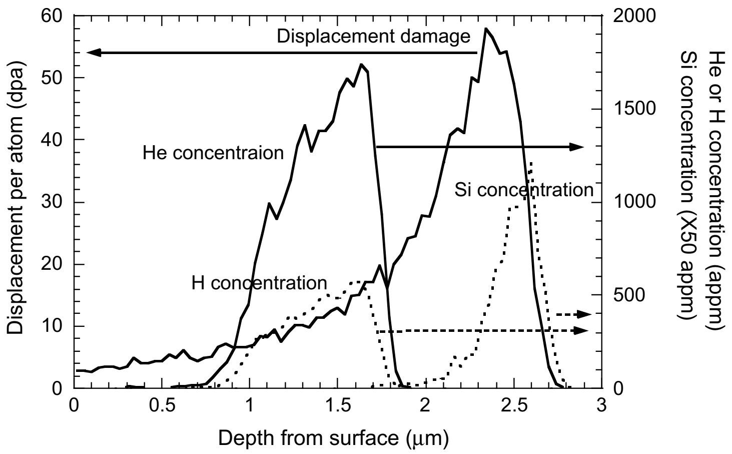

Fig. 1. Displacement damage, He, H and Si concentration as a function of depth from the surface in SiC calculated by TRIM code.

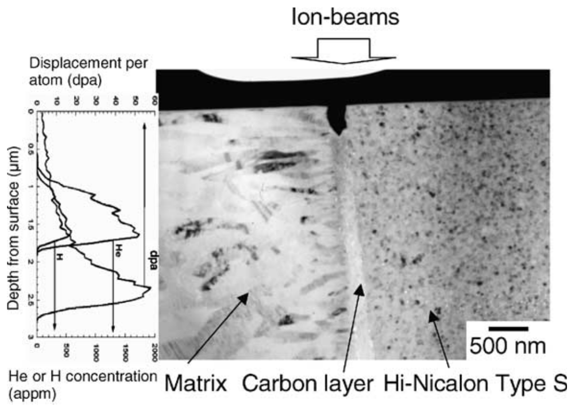

Fig. 2. Low-magnification TEM microphotograph of the irradiated SiC/SiC composite by simultaneous triple ion-beams at 1300 °C.

advanced SiC fiber and matrix are same step height in Fig. 2. This result indicates that the shrinkage of advanced SiC fibers did not occur. The apparent reason for this is that the advanced SiC fibers consist of near-stoichiometry and highly crystalline SiC structure [14]. The SiC/SiC composites using advanced SiC fiber appear to have excellent dimensional stability against simultaneous ions irradiation up to 1300 °C.

Cross-sectional TEM microphotographs of the irradiated SiC matrices at about 1.4 μm depth from the surface are given in Fig. 3. The average size, average number density and formation position of He bubbles in the matrix is summarized in Table 2. For implantation at 1000 °C, He bubbles are not observed in the matrix irradiated by single Si ions or single He ions. However, He bubbles were observed in the matrix irradiated under dual (Si + He) or triple (Si + He + H)

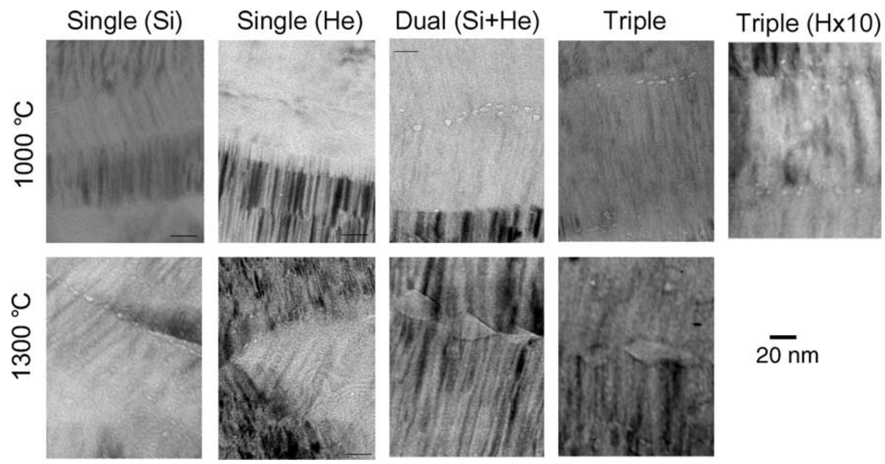

Fig. 3. Cross-sectional TEM microphotographs of the irradiated SiC matrices at about 1.4 μm depth from the surface.

Table 2
Summary of average size, average number density and formation position of He bubbles formed in the matrix

Irradiation temperature (°C)	Condition ID	Single (Si)	Single (He)	Dual (Si + He)	Triple	Triple (×10 H)
	Position	Average size (nm)				
1000	Grain boundary	–	–	4.9	4.6	2.7
	Grain interior	–	–	–	–	–
	Density (m^{-3})	0	0	1.61×10^{22}	2.51×10^{22}	2.75×10^{22}
1300	Grain boundary	5.8	2.3	23.2	20.9	Not examined
	Grain interior	–	–	4.1	3.9	Not examined
	Density (m^{-3})	Not measured	Not measured	5.92×10^{22}	7.22×10^{22}	Not examined

ion-beams. These results reveal that the simultaneous ion-beams irradiation enhances the formation of stable He clusters. It is thought that this is caused by the simultaneous formation of vacancies by the silicon ion damage that are stabilized in the presence of helium. Once stable vacancy clusters are formed they continue to add helium leading the observed helium bubbles. These He bubbles were preferentially formed at the grain boundaries. The average size of He bubbles decreased with increasing amount of implanted H ions. On the other hand, the number density of He bubbles slightly increased with increasing the amount of implanted H ions. These results indicate that the simultaneous implanted H might prevent the migration of He and the growth of He bubbles might be inhibited. Hojou has reported that H atoms implanted simultaneously with He atoms would contribute to forming a large number of nuclei for bubbles formation at room temperature by in-situ TEM observation technique [15]. The result in this study is corresponding to this previous work.

At irradiation temperature of 1300 °C, He bubbles were observed in the matrix irradiated by single He ions, dual and triple ion-beams. Hasegawa has reported that He bubbles were formed in He pre-implanted matrix of SiC/SiC composite annealed at 1400 °C for 1 h [16]. Such voids (average size: 5.8 nm) were also observed in the matrix irradiated by single Si ions although gas atoms such as He and H were not implanted. Price reported that neutron irradiation at 1250 °C produces voids in β-SiC and the average size of voids was 4.2 nm [17]. The results in this study are in good agreement with the previous studies. Helium bubbles in the matrix irradiated by single He ions and the voids were mainly formed at grain boundaries. Helium bubbles in the matrix irradiated by dual and triple ion-beams were formed both at grain boundaries and within the grains. The average size of He bubbles at the grain boundary was much larger than that in the grain. The reason is that the recombination of He clusters was accelerated since the mobility of He interstitial and vacancy at grain boundary is larger than that in the grain.

Large He bubbles were not, however, formed at the grain boundary near carbon fiber/matrix interphase layer. The cross-sectional TEM microphotograph of the irradiated matrix near the carbon layer by simultaneous triple ion-beams at 1300 °C is given in Fig. 4. The number of grain boundaries in the matrix near carbon layer was larger than that in the matrix far from carbon layer since the grain size of the matrix near the carbon layer was smaller as compared to that of matrix far from carbon layer. The large number of grain boundaries might accelerate the release of He from SiC because the mobility of He at the grain boundary is larger than that within the SiC grains. It is, therefore, easier for He to diffuse in matrix near carbon layer compared to the matrix far form carbon layer. Furthermore, Jung has reported the magnitude of the diffusion coefficient of He in graphite to be about 30 times greater than that of SiC [18]. From this result, He in the carbon layer appears to have been released during the ion irradiation at 1300 °C and He in the SiC matrix near the carbon layer also would seem to have been released from the SiC easily. Therefore, the large He bubbles were not formed at the grain boundary of matrix near carbon layer.

At grain boundary in the matrix, the number density of He bubbles at 1300 °C is smaller than that at 1000 °C

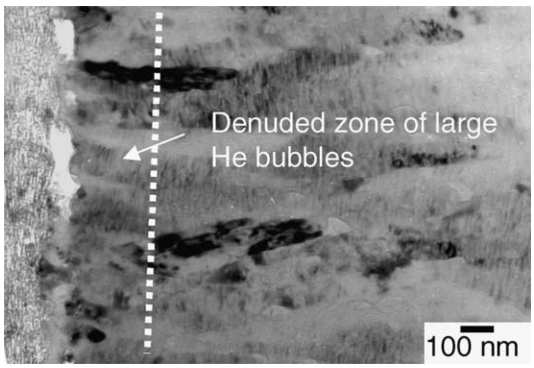

Fig. 4. Cross-sectional TEM microphotograph of the irradiated matrix near carbon layer by simultaneous triple ion-beams at 1300 °C.

while average size of He bubbles is much larger than that at 1000 °C (see Fig. 3). The reason for bubbles size is that much more He clusters go into the grain boundary at 1300 °C compared to the case of 1000 °C since the mobility of He cluster at 1300 °C is much larger than that at 1000 °C.

He bubbles formed at irradiation temperature of 1000 °C were observed only in the He implanted region (0.7–1.8 μm from the surface). On the other hand, He bubbles at 1300 °C were also observed outside of He implanted region; the formation depth-range of He bubbles was from 0 to 3.0 μm. The mobility of He interstitial and induced vacancy was increased with increasing the irradiation temperature. Therefore, He bubbles grew easily and the number of visible He bubbles was increased at higher temperature.

The cross-sectional TEM microphotographs of the irradiated Hi-Nicalon Type S and Tyranno SA SiC fiber at about 1.4 μm depth from the surface were shown in Figs. 5 and 6. The advanced SiC fibers have a different

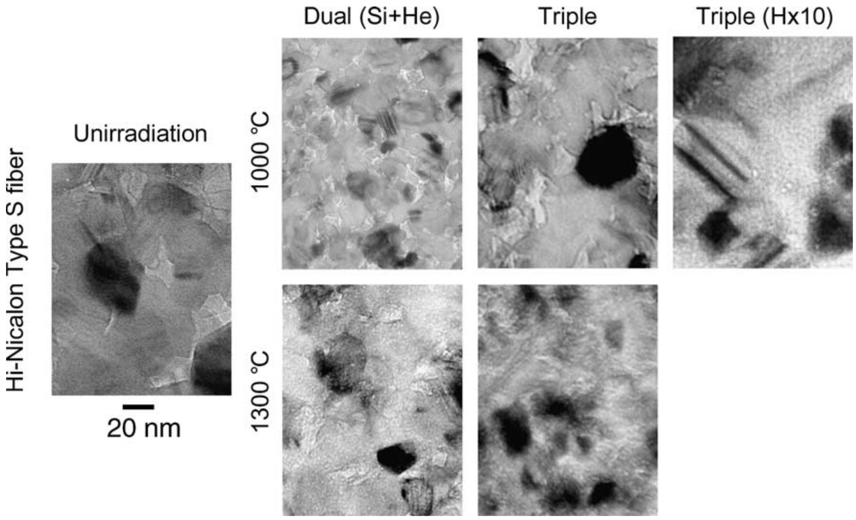

Fig. 5. Cross-sectional TEM microphotographs of the irradiated Hi-Nicalon Type S SiC fiber at about 1.4 μm depth from the surface.

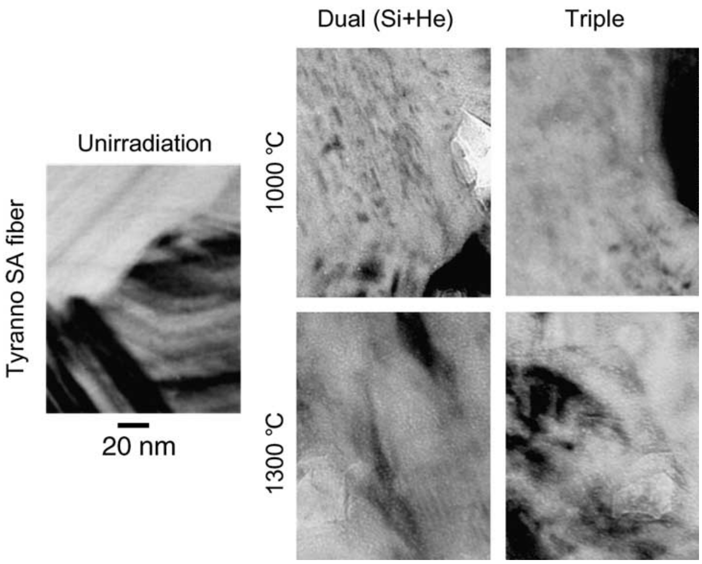

Fig. 6. Cross-sectional TEM microphotographs of the irradiated Tyranno SA SiC fiber at about 1.4 μm depth from the surface.

Table 3
Average size of He bubbles formed in SiC fiber

Irradiation temperature (°C)	Kind of SiC fiber	Condition ID		
		Dual (nm)	Triple (nm)	Triple (H × 10)
1000	Hi-Nicalon Type S	–	2.6	3.0 nm
	Tyranno SA	2.3	2.2	Not examined
1300	Hi-Nicalon Type S	2.5	2.3	Not examined
	Tyranno SA	2.5	3.0	Not examined

microstructure from the matrix. The matrix was dense while the fibers were slightly porous; the density of CVD–SiC is 3.2 g/cm^3 while that of advanced SiC fibers is 3.1 g/cm^3 [19,20]. White contrast areas, whose size is much larger than that of He bubbles, were observed among the grains in the fiber (as shown in Figs. 5 and 6). On the other hand, such white areas were not observed among the grains in the matrix. These white contrast areas are seemed to be pore or carbon phase, whose density is smaller than that of SiC. The summary of average size of He bubbles formed in the SiC fiber is given in Table 3. At irradiation temperature of 1000 °C, no He bubbles were formed in Hi-Nicalon Type S irradiated by dual ion-beams. On the other hand, a few He bubbles were formed by triple ion-beams and He bubbles in the matrix irradiated by dual ion-beams at 1000 °C were observed. Furthermore the number density of He bubbles in the fiber was much smaller than that in the matrix. The grain size of Hi-Nicalon Type S fiber is much smaller than that of matrix, and the pore and carbon phase exists among the grains in the fiber as mentioned above. Therefore, He interstitial and induced vacancy easily reached the grain boundary and were trapped in the pore and carbon phase. For the above reasons, no He bubbles were formed in Hi-Nicalon Type S fibers. The average size of He bubbles formed at irradiation temperature of 1300 °C is almost the same as compared to that at 1000 °C. On the other hand, the number density of He bubbles increased with increasing irradiation temperature. The apparent reason for this is that the number of visible He bubbles was increased since the mobility of He interstitial and vacancy increased with increasing irradiation temperature and the recombination of He clusters was accelerated.

At irradiation temperature of 1000 and 1300 °C, He bubbles were formed in the Tyranno SA SiC fiber irradiated by both dual and triple ion-beams. By dual ion-beams irradiation at 1000 °C, no He bubbles were formed in Hi-Nicalon Type S while a few He bubbles were formed in Tyranno SA fiber. The reason for this is that the number of He interstitials and induced vacancies trapped in the pore among SiC grains were decreased since the grain size of Tyranno SA is larger than that of the Hi-Nicalon Type S, and the distance between pores was also larger. Helium bubbles formed in Tyranno SA fiber are observed both at grain boundary and within the grains. The average size of He bubbles at grain boundary is slightly larger than that in the grains. The average size of He bubbles in Tyranno SA was almost same as that in Hi-Nicalon Type S. The number density of He bubbles was increased with increasing the irradiation temperature as well as Hi-Nicalon Type S.

4. Conclusions

1. The SiC/SiC composites using advanced SiC fiber appear to have excellent dimensional stability against simultaneous triple-ions irradiation at up to 1300 °C with no observed microstructural change occurring at the interphase region.
2. At the irradiation temperature of 1000 °C, He bubbles were not observed in the matrix irradiated by single Si ions or single He ions while He bubbles were observed in the matrix irradiated by dual or triple ion-beams. Simultaneous existence of the induced vacancies by Si ion beam and implanted He ions contributed to the formation of He bubbles.
3. The average size of He bubbles in the matrix decreases with increasing density of implanted H ions. The number density of He bubbles increases when the implantation temperature is increased from 1000 to 1300 °C and the amount of implanted H is increased.
4. At the irradiation temperature of 1000 °C, He bubbles in the matrix were mainly formed near the grain boundary. At the irradiation temperature of 1300 °C, He bubbles in the matrix were formed both at grain boundary and within the grains. The average size of He bubbles at grain boundary was much larger than that near the grain.
5. Under dual ion-beams irradiation at 1000 °C, no He bubbles were formed in Hi-Nicalon Type S while a few He bubbles were formed in Tyranno SA fiber. Helium bubbles were formed in Hi-Nicalon Type S and Tyranno SA by triple ion-beams at 1000 °C and both of dual and triple ion-beams at 1300 °C.

References

[1] L.L. Snead, R.H. Jones, A. Kohyama, P. Fenici, J. Nucl. Mater. 233–237 (1996) 26.

[2] R.H. Jones, D. Steiner, H.L. Heinisch, G.A. Newsome, H.M. Kerch, J. Nucl. Mater. 245 (1997) 87.

[3] P. Fenici, A.J. Frias Rebelo, R.H. Jones, A. Kohyama, L.L. Snead, J. Nucl. Mater. 215 (1998) 258.

[4] A. Hasegawa, A. Kohyama, R.H. Jones, L.L. Snead, B. Riccardi, P. Fenici, J. Nucl. Mater. 283–287 (2000) 128.

[5] R.H. Jones, L. Giancarli, A. Hasegawa, Y. Katoh, A. Kohyama, B. Riccardi, L.L. Snead, W.J. Weber, J. Nucl. Mater. 307–311 (2002) 1057.

[6] T. Hinoki, L.L. Snead, Y. Katoh, A. Hasegawa, T. Nozawa, A. Kohyama, J. Nucl. Mater. 307–311 (2002) 1157.

[7] T. Taguchi, E. Wakai, N. Igawa, S. Nogami, L.L. Snead, A. Hasegawa, S. Jitsukawa, J. Nucl. Mater. 307–311 (1998) 1135.

[8] T. Taguchi, N. Igawa, S. Jitsukawa, T. Nozawa, Y. Katoh, A. Kohyama, L.L. Snead, J.C. McLaughlin, Ceram. Trans. 144 (2002) 69.

[9] J.F. Ziegler, J.P. Biersack, U. LittmarkThe Stopping and Ranges of Ions in Matter, vol. 1, Pergamon, New York, 1985.

[10] R. Devanathan, W.J. Weber, J. Nucl. Mater. 278 (2000) 258.

[11] L.L. Snead, D. Steiner, S.J. Zinkle, J. Nucl. Mater. 191–194 (1992) 566.

[12] L.L. Snead, M.C. Osborne, R.A. Lowden, J. Strizak, R.J. Shinavski, K.L. More, W.S. Eatherly, J. Bailey, A.M. Williams, J. Nucl. Mater. 253 (1998) 20.

[13] S. Nogami, A. Hasegawa, K. Abe, T. Taguchi, R. Yamada, J. Nucl. Mater. 283–287 (2000) 268.

[14] T. Nozawa, L.L. Snead, Y. Katoh, A. Kohyama, J. Nucl. Mater. 329–333 (2004) 544.

[15] K. Hojou, S. Furuno, K.N. Kushita, H. Otsu, K. Izui, Nucl. Instr. and Meth. Phys. Res. B 91 (1994) 534.

[16] A. Hasegawa, M. Saito, S. Nogami, K. Abe, R.H. Jones, H. Takahashi, J. Nucl. Mater. 264 (1999) 355.

[17] R.J. Price, J. Nucl. Mater. 48 (1973) 47.

[18] P. Jung, J. Nucl. Mater. 191–194 (1992) 377.

[19] M. Takeda, A. Urano, J. Sakamoto, Y. Imai, J. Nucl. Mater. 258–263 (1998) 1594.

[20] T. Ishikawa, Y. Kohtoku, K. Kumagawa, T. Yamamura, T. Nagasawa, Nature 391 (1998) 773.